Role of charge transfer in dehydrogenation of M(NH2BH 3)2 (M = Mg, Sr)

ARTICLE *in* THE JOURNAL OF PHYSICAL CHEMISTRY C · AUGUST 2014

Impact Factor: 4.77 · DOI: 10.1021/jp502493g

4 AUTHORS, INCLUDING:

Qiang Sun
Zhengzhou University
112 PUBLICATIONS **842** CITATIONS
SEE PROFILE

Z. Xiao Guo
University College London
202 PUBLICATIONS **3,960** CITATIONS
SEE PROFILE

THE JOURNAL OF PHYSICAL CHEMISTRY C

Article

pubs.acs.org/JPCC

Role of Charge Transfer in Dehydrogenation of $M(NH_2BH_3)_2$ (M = Mg, Sr)

Peng-Fei Yuan,[†] Qiang Sun,[†] Yu Jia,*[,†] and Z. X. Guo*[,‡]

[†]International Joint Research Laboratory for Quantum Functional Materials of Henan Province, and School of Physics and Engineering, Zhengzhou University, Henan 450001, China

[‡]Department of Chemistry/London Center for Nanotechnology, University College London, London WC1H 0AJ, United Kingdom

Supporting Information

ABSTRACT: The dehydrogenation mechanism of $M(NH_2BH_3)_2$ (M = Mg, Sr) was studied by a first-principles method. The results show that the gas-phase energy barrier for the first H_2 release is 2.15 eV via a N−H···B transition state and 1.35 eV via a Mg···H transition state for the second H_2 release in $Mg(NH_2BH_3)_2$. The barrier is 1.21 and 2.27 eV via a N−H···B transition state for the first and second H_2 release in $Sr(NH_2BH_3)_2$, respectively. For the dimer, both compounds release the first H_2 via oligomerization and the corresponding barriers are 1.01 eV for $Mg(NH_2BH_3)_2$ and 1.25 eV for $Sr(NH_2BH_3)_2$. Further analysis of the charges of the transition states and the initial states leads to a general conclusion: for the same final state, the smaller the charge transfer, the lower the barrier. For $Mg(NH_2BH_3)_2$, the reaction pathway is determined by the HOMO and LUMO orbitals of the initial state.

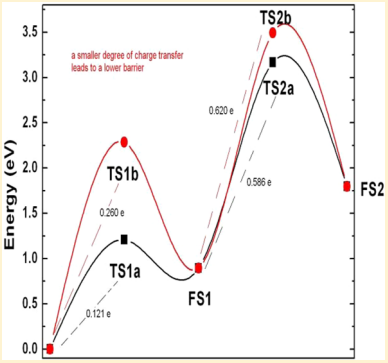

1. INTRODUCTION

Hydrogen storage is an important issue for hydrogen fuel cell vehicles.[1] NH_3BH_3 has a 19.6 wt % storage capacity and is an attractive material, which has been studied for many years.[2] The first two H_2 can be released at ∼110 and 150 °C, respectively.[3−6] However, the direct use of this material has been unsuccessful because of its poor dehydrogenation kinetics and unwanted byproducts.[2,7,8] Various methods have been used to improve its properties, such as chemical doping with transition metals,[9,10] catalysts,[11,12] and ionic liquids.[13] Because these additions do not release hydrogen at the operating temperature, the overall hydrogen storage capacity is reduced. Recently, the substitution of one H(N) [H(N) denotes a H atom bound to N] atom by a metal atom has been investigated. Under this condition, both the kinetics and the thermodynamics can be improved and unwanted byproducts are suppressed.[14−19] The studied metals have all been alkali metals or alkali-earth metals. Some researchers even found that bimetal substitution is superior to single-metal substitution. Although these improvements are advantageous, a drawback of these metal amidoboranes is irreversibility. To overcome this, further understanding of the reaction mechanism is required and computational simulations can offer great insights toward this goal.

Previous studies have focused on NH_3BH_3 and $LiNH_2BH_3$, and it has been found that H_2 is released via a N−H···B transition state in NH_3BH_3 and via a Li···H transition state in $LiNH_2BH_3$ in the gas phase.[20−24] For the dimer, the mechanism is more complex. However, these studies have only concentrated on the reaction pathway or barrier and did not consider the relationship between the initial state and the reaction pathway. Previous studies on small particles, especially clusters, have shown that correlations exist between structure and reactivity.[25,26] In a recent paper, correlations in the oxygen reduction reaction activity of different transition metal catalysts were studied.[27] Their results showed that the binding energy of atomic oxygen can serve as a useful parameter to describe the catalytic activity of pure metals on oxygen reduction. Therefore, there exists a correlation between the initial state of a hydrogen containing molecule and its reaction pathway and a question arises about how to determine this correlation. Our previous study on $Ca(NH_2BH_3)_2$ showed that charge transfer between the transition state and the initial states is an important parameter,[28] but it is not known if the same also applies to other metal amidoboranes. In this paper we aim to clarify this issue for $Mg(NH_2BH_3)_2$ and $Sr(NH_2BH_3)_2$.

First, the dehydrogenation barriers of $Mg(NH_2BH_3)_2$ and $Sr(NH_2BH_3)_2$ in the gas phase and as dimers were studied. Charge transfer between the transition state and the initial state was then investigated. Our results show that charge transfer is an important parameter to describe the correlation between the initial states and the reaction barrier. In addition, other useful parameters that could be used to determine the reaction pathway are also discussed.

Received: March 12, 2014
Revised: July 21, 2014
Published: July 22, 2014

dx.doi.org/10.1021/jp502493g | J. Phys. Chem. C 2014, 118, 18315−18324

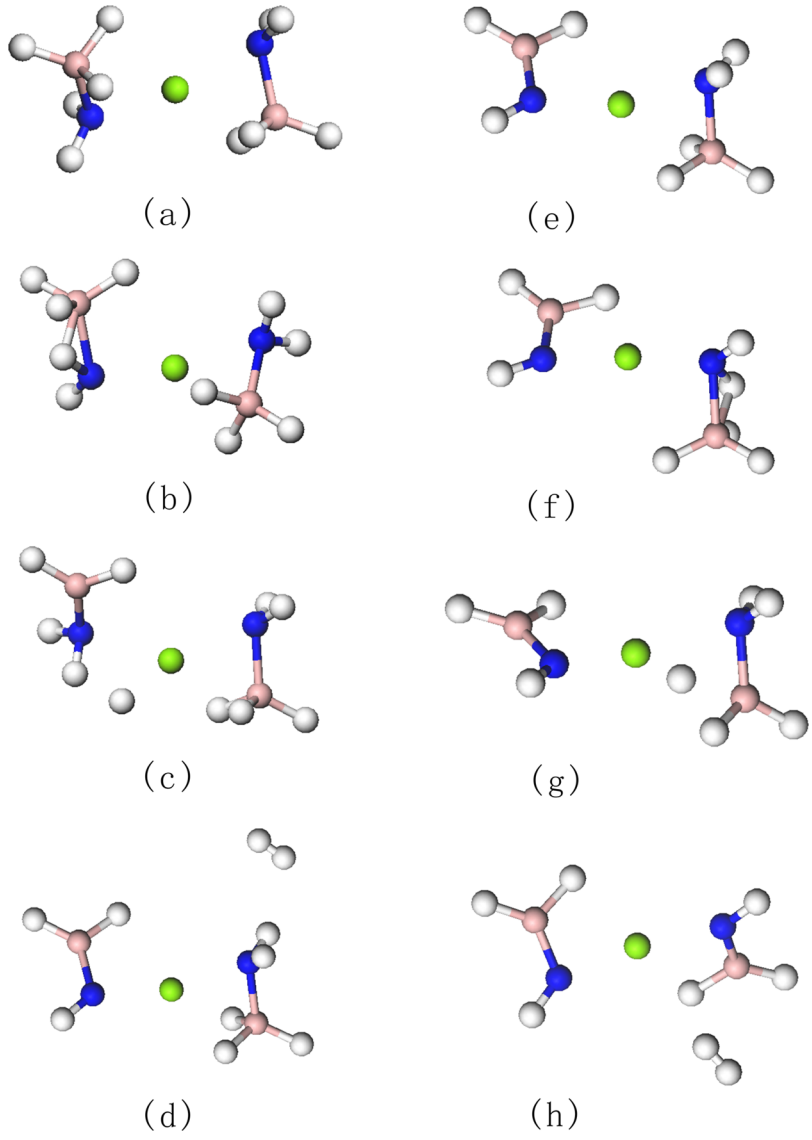

Figure 1. Relaxed molecular structures of $Mg(NH_2BH_3)_2$: (a) initial state, (b) transition state TS1a, (c) transition state TS1b, (d) final state FS1, (e) initial state after the first H_2 is released, (f) transition state TS2a, (g) transition state TS2b, and (h) final state FS2. Green, pink, blue, and white spheres denote Mg, B, N, and H atoms, respectively.

2. COMPUTATIONAL METHODS

First-principles calculations were carried out within the density functional theory framework.[29] The projector-augmented wave (PAW) method[30,31] and the generalized gradient approximation (GGA)[32] for the exchange-correlation energy functional, as implemented in the Vienna ab initio simulation package (VASP),[33−35] were used. The GGA calculation was performed with the Perdew−Burke−Ernzerhof (PBE)[36] exchange-correlation potential. Simulation cells 15 × 15 × 15 $Å^3$ in size were used for the isolated molecule and 20 × 20 × 20 $Å^3$ for the dimers. A plane-wave cutoff energy of 400 eV was used. The Nudged Elastic Band (NEB) method[37] was used to determine the minimum energy pathway. All atoms were fully relaxed with a tolerance in total energy of 0.01 meV, and the forces on each atom were less than 0.01 eV/Å. Atomic charges were calculated by a Bader charge analysis[38] for all processes.

3. RESULTS AND DISCUSSION

3.1. Dehydrogenation Barrier of $Mg(NH_2BH_3)_2$. To determine the dehydrogenation mechanism of $Mg(NH_2BH_3)_2$, we first studied the basic properties of this material in the gas phase. The optimized structure is shown in Figure 1a, and the relevant bond lengths and bond angles are listed in Table S1 (Supporting Information). This structure is similar to $Ca(NH_2BH_3)_2$, and so are the bond lengths and bond angles.[28] Experimentally, dehydrogenation occurs in the solid phase and, therefore, the behavior of the nearby molecules must be considered. Here, we used a dimer to express this effect. The optimized structure of the $Mg(NH_2BH_3)_2$ dimer is shown in Figure 2a, and the bond lengths and bond angles are listed in Table S2 (Supporting Information). The dimer structure is similar to the $Ca(NH_2BH_3)_2$ dimer and so are the bond lengths and bond angles. Having obtained the basic properties of the monomer and the dimer, we calculated the dehydrogenation barriers of the different pathways. Some points of note are the following: (1) Compared with $LiNH_2BH_3$, $Mg(NH_2BH_3)_2$

dx.doi.org/10.1021/jp502493g | J. Phys. Chem. C 2014, 118, 18315−18324

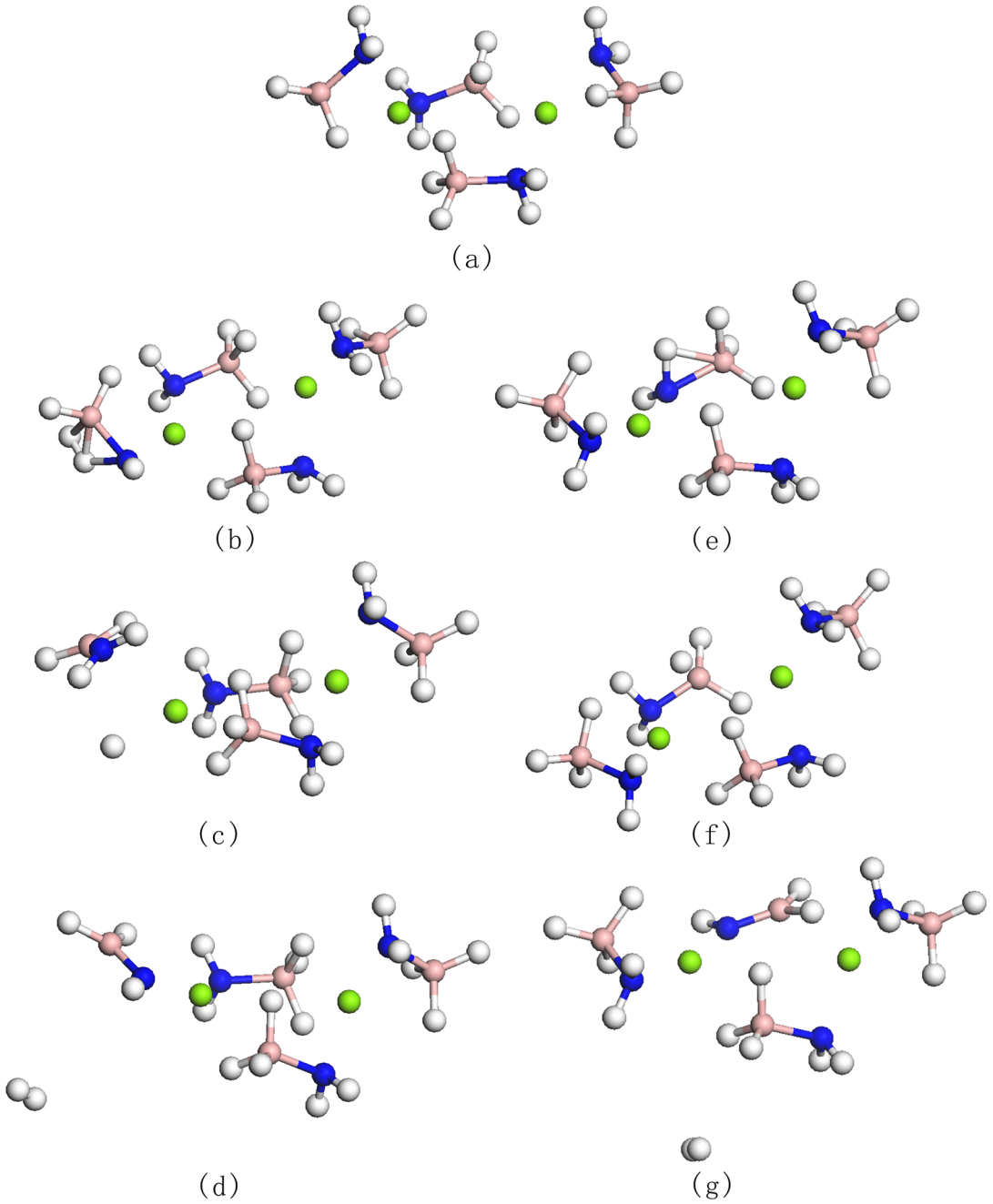

Figure 2. Relaxed molecular structures of the $Mg(NH_2BH_3)_2$ dimer: (a) initial state, (b) transition state TSd1a, (c) transition state TSd1b, (d) final state FSd1, (e) transition state TSd2a, (f) transition state TSd2b, and (g) final state FSd2. Green, pink, blue, and white spheres denote Mg, B, N, and H atoms, respectively.

contains two $[NH_2BH_3]^-$ groups and H_2 can be released from either one or both of them upon oligomerization. (2) Two different dehydrogenation pathways were considered, one via a N−H···B transition state (the transition state of NH_3BH_3 dehydrogenation) and the other via a Mg···H transition state (the transition state of $LiNH_2BH_3$ dehydrogenation). (3) For the dimer, the four $[NH_2BH_3]^-$ groups can be divided into two subgroups: the $[NH_2BH_3]^-$ side group, which is only linked to one Mg atom; and the $[NH_2BH_3]^-$ bridging group, which is linked to two Mg atoms. The final state energy after H_2 release and the corresponding barrier are identical, respectively, for the two $[NH_2BH_3]^-$ in the same subgroup, but different for different subgroups. Therefore, for the first H_2 release from the dimer we calculated four different pathways (each subgroup has two different pathways).

The obtained energy barriers of the monomer and dimer for the different pathways are shown in Figure 3. The corresponding structures of the transition states and the final states are shown in Figures 1b−h and 2b−g, respectively. The bond lengths and bond angles are listed in Tables S1 and S2 (Supporting Information), respectively. For the monomer, the energy of the final state FS1 (the final state after the first H_2 release) is 0.82 eV higher than the initial state, and the energy of the final state FS2 (the final state after the second H_2 release) is 0.84 eV higher than FS1. The energy barrier is 2.15 eV via the N−H···B transition state (TS1a) and 2.19 eV via the

dx.doi.org/10.1021/jp502493g | J. Phys. Chem. C 2014, 118, 18315−18324

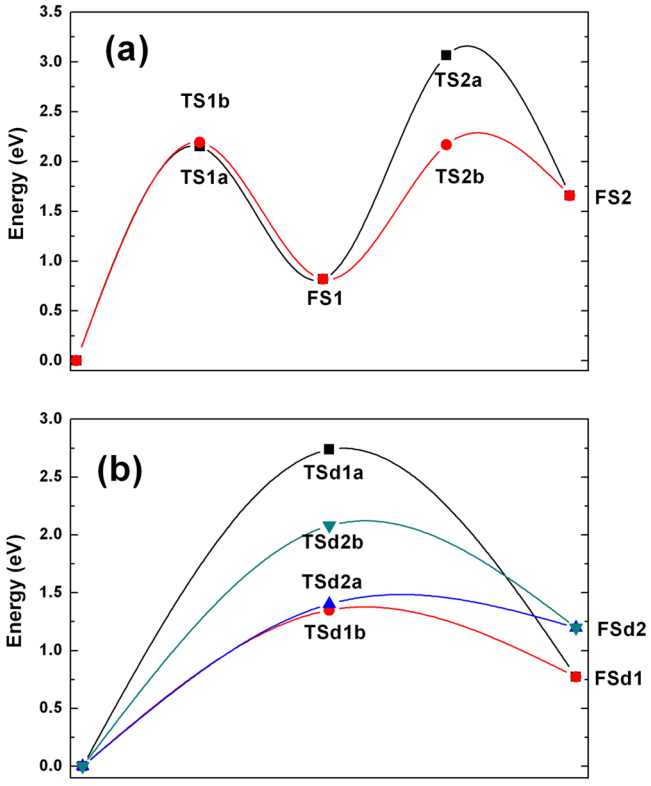

Figure 3. (a) Schematic electronic energy profiles for the first and second H_2 release from $Mg(NH_2BH_3)_2$ via different transition states. The energy of $Mg(NH_2BH_3)_2$ was set to zero. Lines are drawn as a guide. (b) Schematic electronic energy profiles for H_2 release from the $Mg(NH_2BH_3)_2$ dimer to two different final states (FSd1 and FSd2), each via two different transition states (TSd1a, TSd1b and TSd2a, TSd2b). The energy of the $Mg(NH_2BH_3)_2$ dimer was set to zero. Lines are drawn as a guide.

Mg···H transition state (TS1b) for the first H_2 release, and the barrier is 2.25 eV via the N−H···B transition state (TS2a) and 1.35 eV (both compared with the energy of FS1) via the Mg···H transition state (TS2b) for the second H_2 release, respectively. The oligomerization barrier was also calculated. The calculated barrier is 3.35 eV and the energy of the final state is 1.81 eV higher than that of the initial state. Therefore, the oligomerization process is both energetically and kinetically unfavorable in the monomer and we will not discuss this process further.

In ref 23, the barrier of the Mg···H pathway and the oligomerization pathway were also calculated. The relevant barriers are 1.57 and 1.98 eV (both compared with the energy of $Mg(NH_2BH_3)_2$) for the first and second H_2 release via the Mg···H pathway, respectively, and the barriers are 2.00 and 2.07 eV via the oligomerization pathway, respectively. Our results indicate higher energies than the reported results but the trend is the same. For the dimer, the FSd1 energy (the final state after H_2 is released from the side $[NH_2BH_3]^-$) is 0.77 eV higher than the initial state, and the FSd2 energy (the final state after H_2 is released from the bridging $[NH_2BH_3]^-$) is 1.20 eV higher than the initial state. The corresponding energy barrier is 2.74 eV via a N−H···B transition state (TSd1a) and 1.35 eV via a Mg···H transition state (TSd1b) to a final state FS1. The energy barrier is 1.40 eV via a N−H···B transition state (TSd2a) and 2.08 eV via a Mg···H transition state (TSd2b) to a final state FS2. In the dimer, oligomerization should occur between the two bridging $[NH_2BH_3]^-$ subgroups because of the shortest H(N)−H(B) distance, 2.486 Å, between the two $[NH_2BH_3]^-$ subgroups. The calculated energy of this final state is 0.53 eV higher than the initial state and the corresponding barrier is 1.01 eV. Therefore, the oligomerization process is both energetically and kinetically more favorable than the others considered in the paper. The reason is discussed in a later section. At the very start, the synthesis of $Mg(NH_2BH_3)_2$[39] was unsuccessful, but $Mg(NH_2BH_3)_2{\cdot}NH_3$ can be obtained.[39] Recently, $Mg(NH_2BH_3)_2$ has been synthesized.[40] The peak temperature of the first dehydrogenation step is about 104 °C, and the corresponding activation energy is about 0.87 eV (84 kJ/mol). The major boron species in the final products is present in tricoordinated BN_3 or BN_2H environments. This means the formation of a new B−N bond, in other words oligomerization process should occur. The calculated barrier of the oligomerization process is 3.35 eV in the monomer and 1.01 eV in the dimer. This indicated the strong effect of the neighbors. So we hope the barrier can be equal to or even smaller than the experimental result of 0.87 eV with increasing the amounts of the neighbors. But for commercial applications as hydrogen storage materials, significant improvement of their dehydrogenation rates is still required.

In our previous work on $Ca(NH_2BH_3)_2$[28] we found that for the same final state, charge transfer between the transition state and the initial state determines the energy barrier, and that a smaller level of charge transfer leads to a lower barrier. Therefore, in this work we calculated the charges of the different states. The results of the monomer are listed in Table 1 and the results of the dimer are listed in Table 2. Therefore, the extent of charge transfer between the different initial states and the transition states was obtained. The calculated value is 0.213e for TS1a and 0.260e for TS1b, 0.172e for TS2a and

Table 1. Calculated Bader Charges (with respect to the neutral atom) for the Initial State, Transition States, and Final States of the $Mg(NH_2BH_3)_2$ Monomer at the Different H_2 Release Steps

	step 1				step2			
	IS1	TS1a	TS1b	FS1	IS2	TS2a	TS2b	FS2
Mg	+1.643	+1.643	+1.597	+1.641	+1.642	+1.641	+1.622	+1.645
B	+1.653	+1.714	+1.859	+1.818	+1.695	+1.700	+1.662	+1.817
N	−1.589	−1.707	−1.685	−1.836	−1.607	−1.721	−1.600	−1.850
H(B)	−0.524	−0.545	−0.552	−0.578	−0.556	−0.540	−0.548	−0.579
	−0.612	−0.493	−0.702	−0.654	−0.625	−0.482	−0.556	−0.655
	−0.614	−0.626	−0.604		−0.610	−0.611	−0.586	
H(N)	+0.446	+0.386	+0.490	+0.426	+0.416	+0.373	+0.423	+0.446
	+0.418	+0.442	+0.434		+0.468	+0.454	+0.414	

dx.doi.org/10.1021/jp502493g | J. Phys. Chem. C 2014, 118, 18315−18324

Table 2. Calculated Bader Charges (with respect to the neutral atom) for the Initial State, Transition States, and Final States of the $Mg(NH_2BH_3)_2$ Dimer[a]

	bridging				nonbridging			
	ISd	TSd1a	TSd1b	FSd1	ISd	TSd2a	TSd2b	FSd2
Mg	+1.628	+1.619	+1.566	+1.624	+1.628	+1.632	+1.639	+1.633
B	+1.659	+1.773	+1.769	+1.812	+1.696	+1.694	+1.692	+1.812
N	−1.636	−1.771	−1.723	−1.834	−1.596	−1.676	−1.665	−1.791
H(B)	−0.587	−0.608	−0.621	−0.649	−0.628	−0.536	−0.521	−0.678
	−0.604	−0.285	−0.666	−0.590	−0.620	−0.681	−0.646	−0.562
	−0.573	−0.552	−0.557		−0.545	−0.548	−0.563	
H(N)	+0.453	+0.413	+0.521	+0.442	+0.459	+0.451	+0.455	+0.411
	+0.467	+0.213	+0.528		+0.430	+0.484	+0.439	

[a]Only the reacted $[NH_2BH_3]^-$ group is listed.

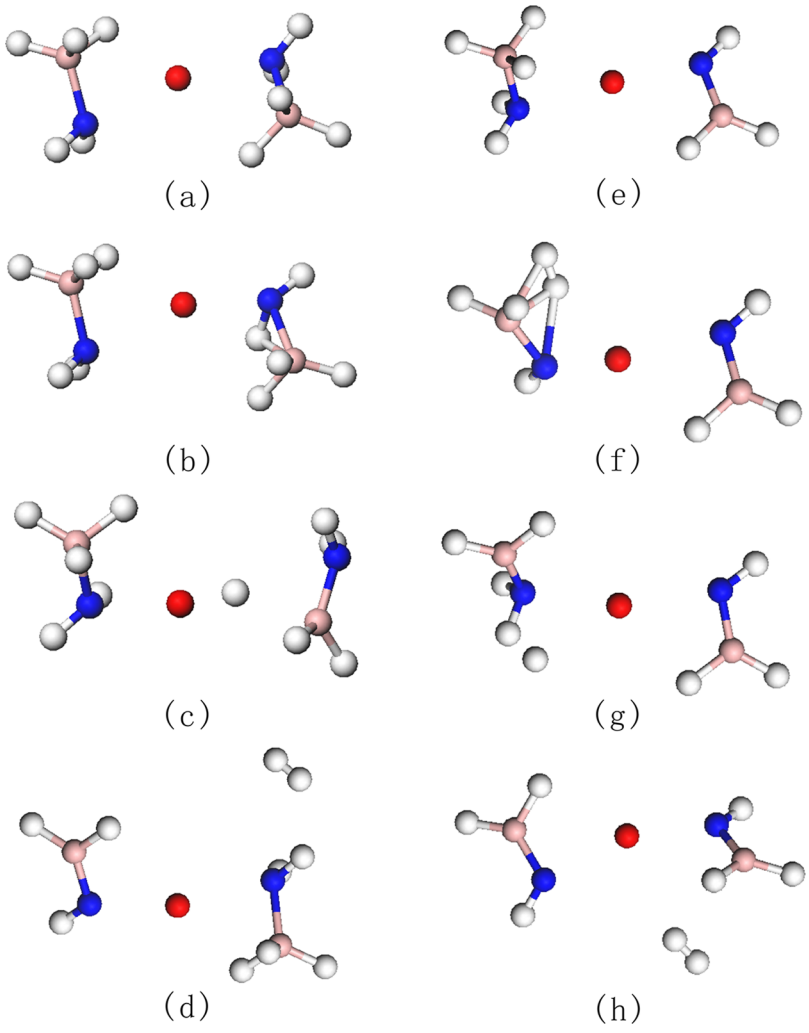

Figure 4. Relaxed molecular structures of $Sr(NH_2BH_3)_2$: (a) initial state, (b) transition state TS1a, (c) transition state TS1b, (d) final state FS1, (e) initial state after the first H_2 is released, (f) transition state TS2a, (g) transition state TS2b, and (h) final state FS2. Red, pink, blue, and white spheres denote Sr, B, N, and H atoms, respectively.

0.108e for TS2b, 0.455e for TSd1a and 0.245 for TSd1b, and 0.155e for TSd2a and 0.122 for TSd2b. Compared with Figure 3, we found that for the monomer a smaller degree of charge transfer leads to a lower barrier, which is the case for the first and the second H_2 release processes. For the dimer, this finding applies to H_2 release from the $[NH_2BH_3]^-$ side group, but not from the $[NH_2BH_3]^-$ bridging group. This is discussed further in section 3.3.

3.2. Dehydrogenation Barrier of $Sr(NH_2BH_3)_2$. As for $Mg(NH_2BH_3)_2$, the dehydrogenation barriers of $Sr(NH_2BH_3)_2$ were calculated for the monomer and the dimer. The corresponding structures for the initial states, transition states, and final states are shown in Figures 4 and 5, and the calculated bond lengths and bond angles are listed in Tables S3 and S4 in the Supporting Information. The energy barriers are shown in Figure 6. From these we can see that the structures are more or

dx.doi.org/10.1021/jp502493g | J. Phys. Chem. C 2014, 118, 18315−18324

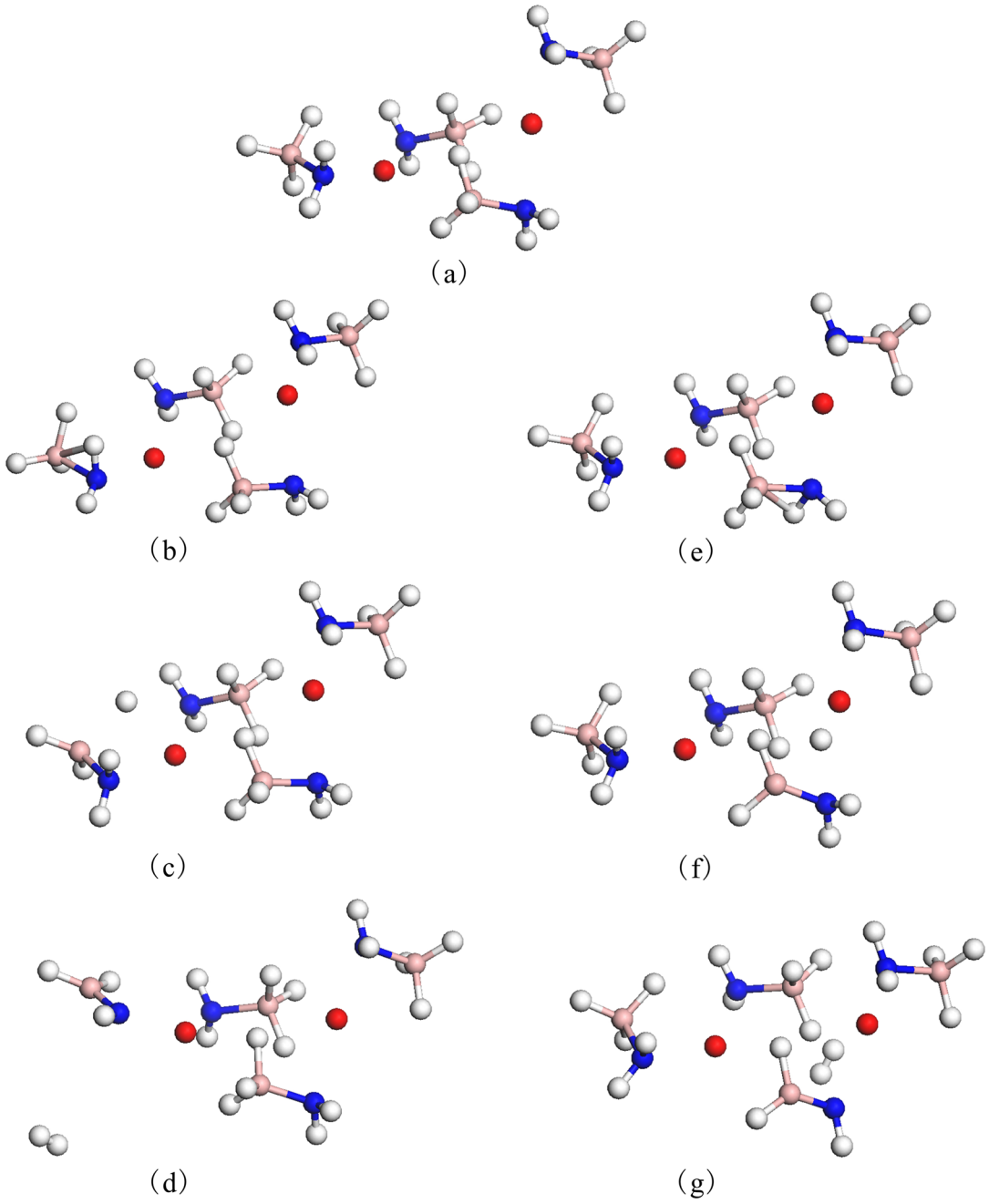

Figure 5. Relaxed molecular structures of the $Sr(NH_2BH_3)_2$ dimer: (a) initial state, (b) transition state TSd1a, (c) transition state TSd1b, (d) final state FSd1, (e) transition state TSd2a, (f) transition state TSd2b, and (g) final state FSd2. Red, pink, blue, and white spheres denote Sr, B, N, and H atoms, respectively.

less the same as those of $Mg(NH_2BH_3)_2$, but some details vary, due mainly to the different ionic radii of Mg and Sr. For the energy barrier, we also considered four different pathways for the monomer and the dimer, as done for $Mg(NH_2BH_3)_2$. For the monomer, the final energy after the first H_2 release (FS1) is 0.90 eV higher than the initial state, and the energy after the second H_2 release (FS2) is also 0.90 eV higher than FS1. The energy barrier is 1.21 eV via a N−H···B transition state (TS1a) and 2.29 eV via a Sr···H transition state (TS 1b) for the first H_2 release, and the barrier is 2.27 eV via a N−H···B transition state (TS2a) and 2.60 eV (both compared with the energy of FS1) via a Sr···H transition state (TS2b) for the second H_2 release. The oligomerization barrier was also calculated as 4.50 eV and the energy of the final state is 1.22 eV higher than that of the initial state. This process is both energetically and kinetically unfavorable and will not be discussed further. For the dimer, the energy of the FSd1 (the final state after H_2 is released from the $[NH_2BH_3]^-$) side group is 1.05 eV higher than the initial state, and the energy of the FSd2 (the final state after H_2 is released from the bridging $[NH_2BH_3]^-$) is 1.34 eV higher than that of the initial state. The corresponding energy barrier is 2.70 eV via a N−H···B transition state (TSd1a) and 1.33 eV via a Sr···H transition state (TSd1b) to the final state FS1, and the energy barrier is 2.11 eV via a N−H···B transition state (TSd2a) and 2.89 eV via a Sr···H transition state (TSd2b) to the final state FS2. In the dimer, the oligomerization process

dx.doi.org/10.1021/jp502493g | J. Phys. Chem. C 2014, 118, 18315−18324

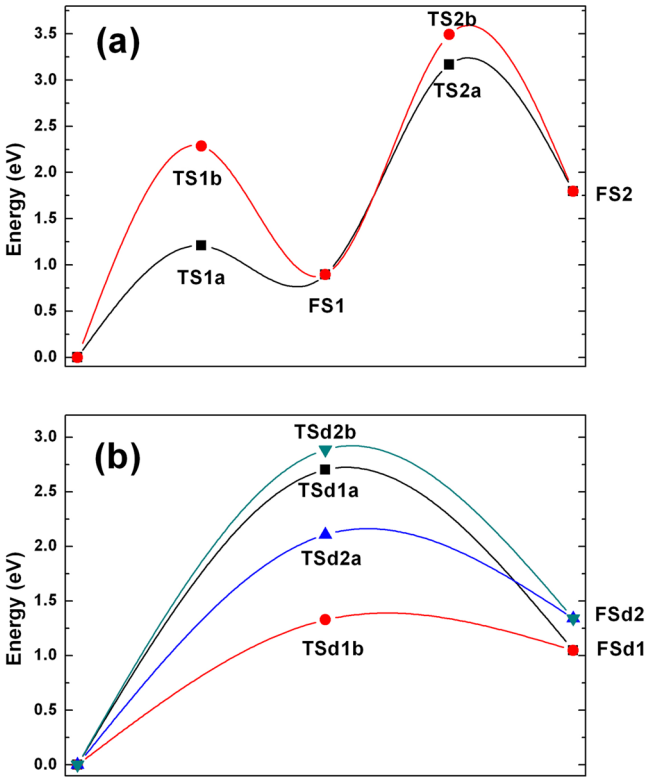

Figure 6. (a) Schematic electronic energy profiles for the first and second H_2 release from $Sr(NH_2BH_3)_2$, via different transition states. The energy of $Sr(NH_2BH_3)_2$ was set to zero. Lines are drawn as a guide. (b) Schematic electronic energy profiles for H_2 release from the $Sr(NH_2BH_3)_2$ dimer to two different final states (FSd1 and FSd2), each via two different transition states (TSd1a, TSd1b and TSd2a, TSd2b). The energy of the $Sr(NH_2BH_3)_2$ dimer was set to zero. Lines are drawn as a guide.

was also considered. The calculated energy of the final state was found to be 0.58 eV higher than that of the initial state and the corresponding barrier is 1.25 eV. Therefore, the oligomerization pathway is both energetically and kinetically more favorable than the others considered in the paper.

We also calculated the Bader charges between the different transition states and the initial states. The results are listed in Tables 3 (monomer) and 4 (dimer). The calculated value is 0.121e for TS1a and 0.210e for TS1b, 0.586e for TS2a and 0.620e for TS2b, 0.086e for TSd1a and 0.163e for TSd1b, and 0.070e for TSd2a and 0.213e for TSd2b. Compared with Figure 6 we found that for the monomer, a smaller degree of charge transfer corresponds to a lower barrier for the first and the second H_2 release processes. For the dimer, this trend only applies to H_2 release from the bridging $[NH_2BH_3]^-$ group, but does not apply to H_2 release from the side $[NH_2BH_3]^-$ group.

3.3. Discussion. From the above observations, we would like to address further the conclusion made previously that "a smaller degree of charge transfer leads to a lower barrier" is not totally correct with regard to the dimer. Two reasons exist. First, in the calculation only the charge transfer in the reacted $[NH_2BH_3]^-$ group was considered. Generally, this relevant group contributes the most to charge transfer. However, sometimes this is not the case. We thus need to consider charge transfer from other adjacent parts of the molecule. When we consider total charge transfer, good agreement is obtained. The charges of each atom are listed in Tables S5 and S6, Supporting Information. For the $Mg(NH_2BH_3)_2$ dimer, the charge transfer values change to 0.340e for TSd2a and 0.386e for TSd2b. For the $Sr(NH_2BH_3)_2$ dimer, the values of charge transfer change to 0.283e for TSd1a and 0.275e for TSd1b. Both can be explained by considering that a smaller level of charge transfer leads to a lower barrier. Furthermore, if we consider the charges of all the atoms in all pathways, this conclusion is still correct. We also found that for the two pathways (TSd2a and TSd2b in $Mg(NH_2BH_3)_2$ and TSd1a and TSd1b in $Sr(NH_2BH_3)_2$), charge transfer of the reacted $[NH_2BH_3]^-$ contributes less to the total charge transfer. Therefore, under this condition, only considering charge transfer from the reacted $[NH_2BH_3]^-$ is not sufficient. Additionally, from the initial state to the transition state the structure shows some change. In our conclusion, we simply considered that the energy change was contributed by electrons. However, structural change also contributes to the energy. Therefore, the energy change can be divided into two parts: one is caused by structural change, E_{str}, and the other by charge transfer, E_{ele}. In most cases, E_{str} is relatively small and is ignored; only E_{ele} is considered. However, if the charge transfer is small, E_{str} should not be neglected. This can be understood by the following assertion: at first, the initial structure changes to a transition structure without a change in the charges of each atom and the electrons of each atom should undergo some degree of exchange during energy minimization. The energy change is E_{str} in the first step and E_{ele} in the second step. Therefore, E_{str} is caused by atoms, and E_{ele} is caused by electrons. The interactions between atoms are mostly van der Waals interactions, and the interactions between electrons are electrostatic interactions. In general, electrostatic interactions are stronger than van der Waals interactions. Therefore, in most cases only considering E_{ele} is sufficient and thus a smaller degree of charge transfer leads to a lower barrier.

Table 3. Calculated Bader Charges (with respect to the neutral atom) for the Initial State, Transition States, and Final States of the $Sr(NH_2BH_3)_2$ Monomer at the Different H_2 Release Steps

	step 1				step2			
	IS1	TS1a	TS1b	FS1	IS2	TS2a	TS2b	FS2
Sr	+1.579	+1.594	+1.488	+1.584	+1.597	+1.585	+1.516	+1.589
B	+1.704	+1.676	+1.772	+1.797	+1.692	+1.835	+1.452	+1.793
N	−1.524	−1.607	−1.620	−1.779	−1.603	−1.784	−1.670	−1.764
H(B)	−0.561	−0.565	−0.582	−0.582	−0.574	−0.565	−0.623	−0.590
	−0.618	−0.621	−0.619	−0.647	−0.602	−0.609	−0.020	−0.645
	−0.604	−0.585	−0.565		−0.605	−0.173	−0.726	
H(N)	+0.423	+0.421	+0.429	+0.419	+0.426	+0.380	+0.365	+0.412
	+0.391	+0.471	+0.475		+0.467	+0.127	+0.496	

dx.doi.org/10.1021/jp502493g | J. Phys. Chem. C 2014, 118, 18315−18324

Table 4. Calculated Bader Charges (with respect to the neutral atom) for the Initial State, Transition States, and Final States of the $Sr(NH_2BH_3)_2$ Dimer[a]

	bridging				nonbridging			
	ISd	TSd1a	TSd1b	FSd1	ISd	TSd2a	TSd2b	FSd2
Sr	+1.577	+1.584	+1.538	+1.578	+1.579	+1.597	+1.538	+1.588
B	+1.722	+1.709	+1.701	+1.752	+1.681	+1.662	+1.699	+1.838
N	−1.564	−1.608	−1.642	−1.752	−1.582	−1.630	−1.653	−1.804
H(B)	−0.632	−0.630	−0.667	−0.652	−0.589	−0.583	−0.482	−0.654
	−0.609	−0.594	−0.601	−0.590	−0.600	−0.615	−0.630	−0.604
	−0.563	−0.575	−0.452		−0.570	−0.575	−0.590	
H(N)	+0.424	+0.431	+0.518	+0.438	+0.439	+0.477	+0.459	+0.434
	+0.435	+0.466	+0.396		+0.433	+0.448	+0.445	

[a]Only the reacted $[NH_2BH_3]^-$ group is listed.

Although this conclusion may be correct in most cases, the reaction barrier should still be calculated and it is always expensive. A question arises about determining the reaction pathway without a barrier calculation. In a recent paper,[41] the authors used HOMO and LUMO orbitals to determine the reaction pathway and they obtained good results. Therefore, we also plotted the HOMO and LUMO orbital of the two studied materials. Those for $Mg(NH_2BH_3)_2$ are shown in Figure 7

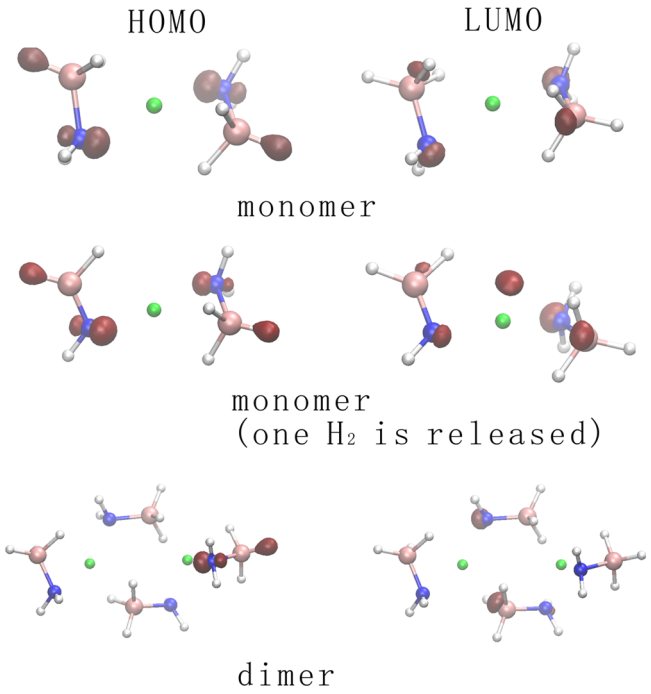

Figure 7. HOMO and LUMO orbitals of the $Mg(NH_2BH_3)_2$ monomer and dimer. Green, pink, blue, and white spheres denote Mg, B, N, and H atoms, respectively.

(initial state, after the first H_2 was released, and the dimer); and those for $Sr(NH_2BH_3)_2$ are shown in Figure S1 in the Supporting Information (initial state, after the first H_2 was released, and the dimer). From Figure 7 we can see that in the initial state the HOMO site is composed of electron wave functions at the N atom and the H(B) atom, and the LUMO site is composed of electron wave functions at the N atom and the B atom, respectively. After the first H_2 is released, the HOMO site is also composed of electron wave functions at the N atom and the H(B) atom, but the LUMO site is composed of electron wave functions at the N atom, the B atom, and the Mg atom. In the dimer, the HOMO site is composed of electron wave functions at the N atom and the H(B) atom in the side $[NH_2BH_3]^-$ group, and the LUMO site is composed of electron wave functions at the N atom and the B atom in the different bridging $[NH_2BH_3]^-$ groups. From these figures, we may assume that the first H_2 is released via a N−H···B process and the second H_2 is released via a Mg···H process in the monomer, and the H_2 is released via oligomerization in the dimer. This agrees well with our previous barrier calculations. However, this does not apply to $Sr(NH_2BH_3)_2$. Therefore, we still need to investigate the relationships between the initial states and the reaction barrier.

4. CONCLUSIONS

Dehydrogenation barriers of $Mg(NH_2BH_3)_2$ and $Sr(NH_2BH_3)_2$ were studied by first-principles simulations. The results show that the first H_2 is released via a N−H···B process and the second H_2 is released via a Mg···H process for the $Mg(NH_2BH_3)_2$ monomer; both the first and the second H_2 are released via a N−H···B process for the $Sr(NH_2BH_3)_2$ monomer. For the dimer, H_2 is released via oligomerization in both materials. From charge analyses of the transition states and the initial states, a general conclusion may be drawn that for the same final state, a smaller degree of charge transfer leads to a lower barrier. Further investigation revealed that for $Mg(NH_2BH_3)_2$, the reaction path can be determined by the HOMO and LUMO orbitals of the initial state but for $Sr(NH_2BH_3)_2$ this does not apply. Therefore, more investigation is required to determine the relationship between its initial state and the reaction pathway.

■ ASSOCIATED CONTENT

Supporting Information

The HOMO and LUMO orbital for $Sr(NH_2BH_3)_2$ monomer and dimer, the calculated bond lengths and bond angles of $Mg(NH_2BH_3)_2$ and $Sr(NH_2BH_3)_2$ monomer and dimer, the calculated Bader charges of $Mg(NH_2BH_3)_2$ and $Sr(NH_2BH_3)_2$ dimer, and the complete author list of authors for refs 7 and14. This material is available free of charge via the Internet at http://pubs.acs.org.

■ AUTHOR INFORMATION

Corresponding Authors

*Tel: +86 371 67739336. E-mail: jiayu@zzu.edu.cn (Y.J.).
*Tel: +44 (0)20 76797527. E-mail: z.x.guo@ucl.ac.uk (Z.X.G.).

Notes

The authors declare no competing financial interest.

■ ACKNOWLEDGMENTS

This work was supported by the Research Fund for the Doctoral Program of Higher Education of China (No. 20124101120009), partly by the "973 project" (No. 2012CB921300), partly by the NSF of China (Grant No. 11274280), and partly by the Program for Innovative Research Team of Science and Technology of Henan Province (Grant No. 2012IRTSTHN003). Z.X.G. is supported by the UK EPSRC (EP/K021192/1, EP/K002252/1). The calculations were performed on the High Performance Clusters of Zhengzhou University.

■ REFERENCES

(1) Graetz, J. New Approaches to Hydrogen Storage. *Chem. Soc. Rev.* **2009**, *38*, 73−82.
(2) Stephens, F. H.; Pons, V.; Tom, B. R. Ammonia−Borane: the Hydrogen Source Par Excellence. *Dalton Trans* **2007**, *25*, 2613−2626.
(3) Sit, V.; Geanangel, R. A.; Wendlandt, W. W. The Thermal Dissociation of NH_3BH_3. *Thermochim. Acta* **1987**, *113*, 379−382.
(4) Hu, M. G.; Geanangel, R. A.; Wendlandt, W. W. The Thermal Decomposition of Ammonia Borane. *Thermochim. Acta* **1978**, *23*, 249−255.
(5) Wolf, G.; Baumann, J.; Baitalow, F.; Hoffman, P. Calorimetric Process Monitoring of Thermal Decomposition of B−N−H Compounds. *Thermochim. Acta* **2000**, *343*, 19−25.
(6) Baitalow, F.; Baumann, J.; Wolf, G.; Jaenicke-Rößler, K.; Leitner, G. Thermal Decomposition of B−N−H Compounds Investigated by Using Combined Thermoanalytical Methods. *Thermochim. Acta* **2002**, *391*, 159−168.
(7) Gutowska, A.; Li, L.; Shin, Y.; Wang, C. M.; Li, X. S.; Linehan, J. C.; Smith, R. S.; Kay, B. D.; Schmid, B.; Shaw, W.; et al. Nanoscaffold Mediates Hydrogen Release and the Reactivity of Ammonia Borane. *Angew. Chem., Int. Ed.* **2005**, *44*, 3578−3582.
(8) Marder, T. B. Will We Soon Be Fueling Our Automobiles with Ammonia−Borane. *Angew. Chem., Int. Ed.* **2007**, *46*, 8116−8118.
(9) Jaska, C. A.; Temple, K.; Lough, A. J.; Manners, I. Transition Metal-Catalyzed Formation of Boron−Nitrogen Bonds: Catalytic Dehydrocoupling of Amine-Borane Adducts to Form Aminoboranes and Borazines. *J. Am. Chem. Soc.* **2003**, *125*, 9424−9434.
(10) Denney, M. C.; Pons, V.; Hebden, T. J.; Heinekey, M.; Goldberg, K. I. Efficient Catalysis of Ammonia Borane Dehydrogenation. *J. Am. Chem. Soc.* **2006**, *128*, 12048−12049.
(11) Keaton, R. J.; Blacquiere, J. M.; Baker, R. T. Base Metal Catalyzed Dehydrogenation of Ammonia−Borane for Chemical Hydrogen Storage. *J. Am. Chem. Soc.* **2007**, *129*, 1844−1845.
(12) Stephens, F. H.; Baker, R. T.; Matus, M. H.; Grant, D. J.; Dixon, D. A. Acid Initiation of Ammonia−Borane Dehydrogenation for Hydrogen Storage. *Angew. Chem., Int. Ed.* **2007**, *46*, 746−749.
(13) Bluhm, M. E.; Bradley, M. G.; Butterick, R.; Kusari, U.; Sneddon, L. G. Amineborane-Based Chemical Hydrogen Storage: Enhanced Ammonia Borane Dehydrogenation in Ionic Liquids. *J. Am. Chem. Soc.* **2006**, *128*, 7748−7749.
(14) Xiong, Z. T.; Yong, C. K.; Wu, G. T.; Chen, P.; Shaw, W.; Karkamkar, A.; Autrey, T.; Jones, M. O.; Johnson, S. R.; Edwards, P. P.; et al. High-Capacity Hydrogen Storage in Lithium and Sodium Amidoboranes. *Nat. Mater.* **2008**, *7*, 138−141.
(15) Wu, H.; Zhou, W.; Yildirim, T. Alkali and Alkaline-Earth Metal Amidoboranes: Structure, Crystal Chemistry, and Hydrogen Storage Properties. *J. Am. Chem. Soc.* **2008**, *130*, 14834−14839.
(16) Xiong, Z. T.; Wu, G. T.; Chua, Y. S.; Hu, J. J.; He, T.; Xu, W. L.; Chen, P. Synthesis of Sodium Amidoborane ($NaNH_2BH_3$) for Hydrogen Production. *Energy Environ. Sci.* **2008**, *1*, 360−363.
(17) Spielmann, J.; Jansen, G.; Bandmann, H.; Harder, S. Calcium Amidoborane Hydrogen Storage Materials: Crystal Structures of Decomposition Products. *Angew. Chem.* **2008**, *120*, 6386−6391.
(18) Himashinie, V. K.; Diyabalanage, R. P. S.; Semelsberger, T. A.; Scott, B. L.; Bowden, M. E.; Davis, B. L.; Burrell, A. K. Calcium Amidotrihydroborate: A Hydrogen Storage Material. *Angew. Chem., Int. Ed.* **2007**, *46*, 8995−8997.
(19) Zhang, Q.; Tang, Ch.; Fang, Ch.; Fang, F.; Sun, D.; Ouyang, L.; Zhu, M. Synthesis, Crystal Structure, and Thermal Decomposition of Strontium Amidoborane. *J. Phys. Chem. C* **2010**, *114*, 1709−1714.
(20) Li, Q. S.; Zhang, J.; Zhang, S. A DFT and ab initio Direct Dynamics Study on the Hydrogen Abstract Reaction of $H_3BNH_3 \rightarrow H_2 + H_2BNH_2$. *Chem. Phys. Lett.* **2005**, *404*, 100−106.
(21) Nguyen, V. S.; Matus, M. H.; Grant, D. J.; Nguyen, M. T.; Dixon, D. A. Computational Study of the Release of H_2 from Ammonia Borane Dimer $(BH_3NH_3)_2$ and Its Ion Pair Isomers. *J. Phys. Chem. A* **2007**, *111*, 8844−8856.
(22) Lee, T. B.; Mckee, M. L. Mechanistic Study of $LiNH_2BH_3$ Formation from $(LiH)_4 + NH_3BH_3$ and Subsequent Dehydrogenation. *Inorg. Chem.* **2009**, *48*, 7564−7575.
(23) Kim, D. Y.; Lee, H. M.; Seo, J. C.; Shin, S. K.; Kim, K. S. Rules and Trends of Metal Cation Driven Hdride-transfer Mechanisms in Metal Amidoboranes. *Phys. Chem. Chem. Phys.* **2010**, *12*, 5446−5453.
(24) Shevlin, S. A.; Kerkeni, B.; Guo, Z. X. Dehydrogenation Mechanisms and Thermodynamics of MNH_2BH_3 (M = Li, Na) Metal Amidoboranes as Predicted from First Principles. *Phys. Chem. Chem. Phys.* **2011**, *13*, 7649−7659.
(25) Sandra, M. L.; Thorsten, M. B. Gas Phase Metal Cluster Model Systems for Heterogeneous Catalysis. *Phys. Chem. Chem. Phys.* **2012**, *14*, 9255−9269.
(26) Dongwon, H.; Sven, N.; Bret, J. Dissociative Chemisorption of Methane on Pt(110)-(1 × 2): Effects of Lattice Motion on Reactions at Step Edges. *J. Phys. Chem. A* **2013**, *117*, 8651−8659.
(27) Yu, T. H.; Hofmann, T.; Sha, Y.; Merinov, B. V.; Myers, D. J.; Heske, C.; Goddard, W. A., III Finding Correlations of the Oxygen Reduction Reaction Activity of Transition Metal Catalysts with Parameters Obtained from Quantum Mechanics. *J. Phys. Chem. C* **2013**, *117*, 26598−26607.
(28) Yuan, P. F.; Wang, F.; Sun, Q.; Jia, Y.; Guo, Z. X. Dehydrogenation Mechanisms of $Ca(NH_2BH_3)_2$: The Less the Charge Transfer, the Lower the Barrier. *Int. J. Hydrogen Energy* **2013**, *38*, 11313−11320.
(29) Kohn, W.; Sham, L. J. Self-Consistent Equations Including Exchange and Correlation Effects. *Phys. Rev.* **1965**, *140*, A1133−1138.
(30) Blöchl, P. E. Projector Augmented-Wave Method. *Phys. Rev. B* **1994**, *50*, 17953−17979.
(31) Kress, G.; Joubert, D. From Ultrasoft Pseudopotentials to the Projector Augmented-Wave Method. *Phys. Rev. B* **1999**, *59*, 1758−1775.
(32) Perdew, J. P.; Wang, Y. Accurate and Simple Analytic Representation of the Electron-Gas Correlation Energy. *Phys. Rev. B* **1992**, *45*, 13244−13249.
(33) Kresse, G.; Hafner, J. Ab initio Molecular Dynamics for Liquid Metals. *Phys. Rev. B* **1993**, *47*, 558−561.
(34) Kresse, G.; Furthmuller, J. Efficient Iterative Schemes for ab initio Total-Energy Calculations Using a Plane-Wave Basis Set. *Phys. Rev. B* **1996**, *54*, 11169−11186.
(35) Kresse, G.; Furthmuller, J. Efficiency of ab-initio Total Energy Calculations for Metals and Semiconductors Using a Plane-Wave Basis Set. *Comput. Mater. Sci.* **1996**, *6*, 15−50.
(36) Perdew, J. P.; Burke, K.; Ernzehof, M. Generalized Gradient Approximation Made Simple. *Phys. Rev. Lett.* **1996**, *77*, 3865−3868.
(37) Henkelman, G.; Uberuaga, B. P.; Jonsson, H. A Climbing Image Nudged Elastic Band Method for Finding Saddle Points and Minimum Energy Paths. *J. Chem. Phys.* **2000**, *113*, 9901−9904.
(38) Henkelamn, G.; Arnaldsson, A.; Jonsson, H. A Fast and Robust Algorithm for Bader Decomposition of Charge Density. *Comput. Mater. Sci.* **2006**, *36*, 354−360.
(39) Chua, Y. S.; Wu, G. T.; Xiong, Z. T.; Karkamkar, A.; Guo, J. P.; Jian, M. X.; Wong, M. W.; Autrey, T.; Chen, P. Synthesis, Structure and Dehydrogenation of Magnesium Amidoborane Monoammoniate. *Chem. Commun.* **2010**, *46*, 5752−5754.

(40) Luo, J. H.; Kang, X. D.; Wang, P. Synthesis, Formation Mechanism, and Dehydrogenation Properties of the Long-Sought $Mg(NH_2BH_3)_2$ Compound. *Energy Environ. Sci.* **2013**, *6*, 1018−1025.
(41) Li, F.; Sun, L. X.; Zhao, J. J.; Xu, F.; Zhou, H. Y.; Zhang, Q. M.; Huang, F. L. Mechanisms of H_2 Generation for Metal Doped $Al_{16}M$ (M = Mg and Bi) Clusters in Water. *Int. J. Hydrogen Energy* **2013**, *38*, 6930−6937.